



HAL
open science

A new protocol for the simultaneous flow cytometric analysis of cytotoxicity and immunotoxicity on zebra mussel (*Dreissena polymorpha*) hemocytes

Iris Barjhoux, Damien Rioult, Alain Geffard, Melissa Palos Ladeiro

► **To cite this version:**

Iris Barjhoux, Damien Rioult, Alain Geffard, Melissa Palos Ladeiro. A new protocol for the simultaneous flow cytometric analysis of cytotoxicity and immunotoxicity on zebra mussel (*Dreissena polymorpha*) hemocytes. *Fish and Shellfish Immunology*, 2019, 10.1016/j.fsi.2019.12.092 . hal-02433472

HAL Id: hal-02433472

<https://hal.science/hal-02433472v1>

Submitted on 7 May 2020

HAL is a multi-disciplinary open access archive for the deposit and dissemination of scientific research documents, whether they are published or not. The documents may come from teaching and research institutions in France or abroad, or from public or private research centers.

L'archive ouverte pluridisciplinaire **HAL**, est destinée au dépôt et à la diffusion de documents scientifiques de niveau recherche, publiés ou non, émanant des établissements d'enseignement et de recherche français ou étrangers, des laboratoires publics ou privés.

A new protocol for the simultaneous flow cytometric analysis of cytotoxicity and immunotoxicity on zebra mussel (*Dreissena polymorpha*) hemocytes

Iris Barjhoux^{a,✉}, Damien Rioult^{a,b}, Alain Geffard^a, Melissa Palos-Ladeiro^a

^a *Université de Reims Champagne-Ardenne, INERIS, SEBIO UMR I02, 51097, Reims, France*

^b *Université de Reims Champagne-Ardenne, INERIS, Plateau technique mobile de cytométrie environnementale MOBICYTE, 51097, Reims, France*

✉ **Corresponding author:** Iris Barjhoux (PhD)

University of Reims Champagne-Ardenne,
UMR-I 02 INERIS-URCA-ULH SEBIO,
UFR SEN, Moulin de la Housse, BP 1039,
51687 Reims Cedex 2, France.

E-mail contact: iris.barjhoux@univ-reims.fr

Phone/Fax: +33 (0)326913719/+33 (0)326913342

Competing interests statement: the authors have no competing interests to declare.

Highlights

- Cell detachment enhances the representativity of the analyzed cell population
- The triple labeling procedure improves the accuracy of measured endpoints
- Hemocyte adhesion ability is used to select functional cells for further analysis
- Hemocyte adhesion is a key property to consider before flow analyses

1 Abstract

2 Immunotoxicity analysis receives a strong interest in environmental *a priori* and *a posteriori* risk assessment
3 procedures considering the direct involvement of the immune system in the health status of organisms,
4 populations and thus ecosystems. The freshwater mussel *Dreissena polymorpha* is an invasive species widely
5 used in ecotoxicology studies and biomonitoring surveys to evaluate the impacts of contaminants on aquatic
6 fauna. Bivalve hemocytes are the immunocompetent cells circulating in the open circulatory system of the
7 organism. However, there is nowadays no consensus on a protocol to evaluate the immunocompetent state of
8 this particular cell type using flow cytometry. Wild species such as *D. polymorpha* present several technical
9 barriers complicating their analyze including (i) the quality and the purity of the hemolymph sample, (ii) the
10 controversial characterization of hemocyte subpopulations and their diversity, (iii) the quantity of biological
11 material, and (iv) the high inter-individual variability of hemocyte responses. The present work proposes several
12 technical and analytical improvements to control the above-mentioned issues. The inclusion of sedimentation and
13 cell detachment steps in the pre-analytical phase of the protocol substantially ameliorate the quality of the
14 hemolymph sample as well as the accuracy of the cytometric measurements, by selecting the analyzed cells on
15 their adhesion ability and by increasing the concentration of the analyzed events. The development of an effective
16 triple-labeling procedure including the cellular probe Hoechst[®] 33342, the membrane impermeant dye propidium
17 iodide and yellow-green fluorescent microspheres allowed the simultaneous analysis of cytotoxicity and
18 phagocytosis activity in hemocytes. It also significantly enhanced the accuracy of hemocyte endpoint
19 measurements by eliminating non-target events from the analysis and allowing relevant gating strategies. Finally,
20 the use of pooled samples of hemolymph noticeably reduced inter-sample variability while providing more
21 plasticity in the experimental design and improving the discriminating potency between treatments. The
22 developed protocol is suitable for *ex vivo* exposure of hemocyte in a chemical/environmental toxicity assessment
23 as well as for *in vivo* exposure in the laboratory or *in situ* biomonitoring surveys with few adaptations.

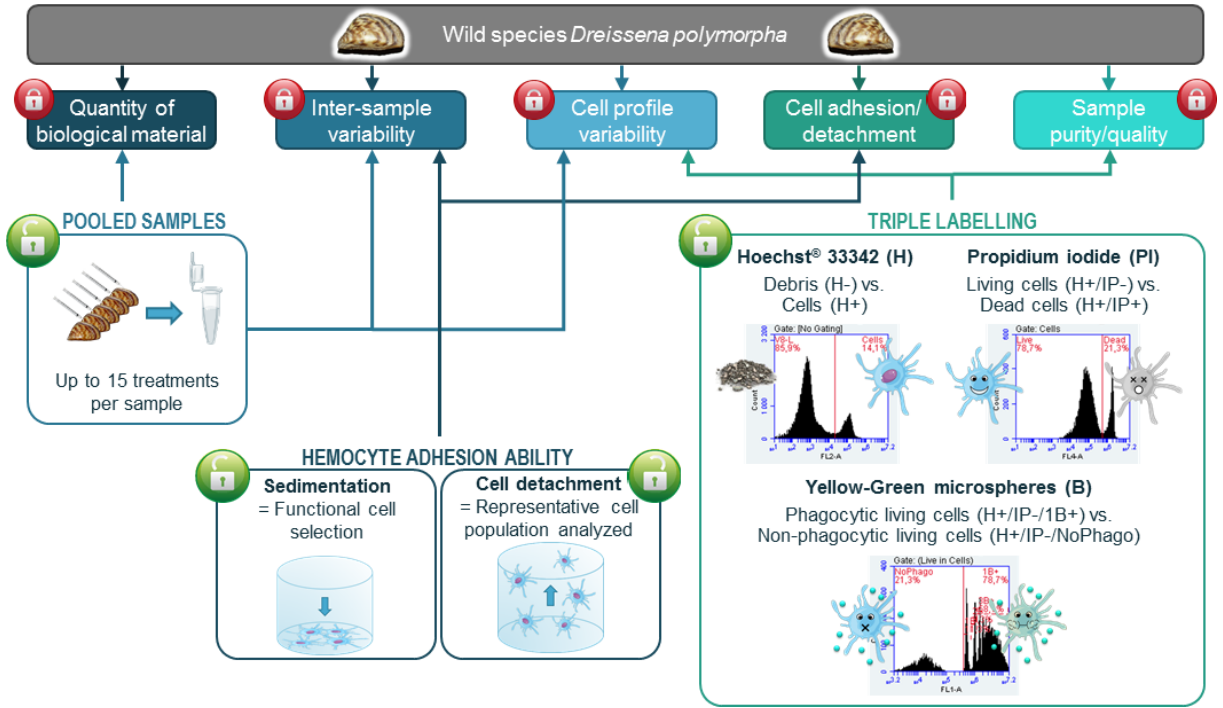
24

25 *Keywords:*

26 Immune cells; wild species; triple labeling; bivalve; phagocytosis; adhesion

27

28 **Graphical Abstract**



29

30

31 1 Introduction

32 The evaluation of immunotoxicity is an important aspect of chemical hazard evaluation and environmental risk
33 assessment processes. Several regulations support this status considering that immune system suppression has
34 been associated with increased incidences of infections and neoplasia (e.g. European Commission (EC), 2006;
35 US EPA, 2007). In invertebrates, which represent more than 90% of the extant aquatic species (Binelli et al.,
36 2009), the immune defense system exclusively relies on innate humoral and cellular strategies principally
37 ensured by the hemocytes, circulating cells in the hemolymph with high tissue infiltration capacities (Tryphonas et
38 al., 2005; Le Foll et al., 2010). The open circulatory system of most of the invertebrates including bivalves implies
39 that the hemolymph, and thus hemocytes, are directly exposed to environmental stressors or contaminants, and
40 play a physiological role in toxic material transport as well as in defense mechanisms (Mersch et al., 1996).
41 Evaluation of critical functions of the immune status in bivalves can thus help to determine the relationship
42 between sublethal and/or chronic exposure to environmental contaminants and immunotoxicological effects
43 (Blaise et al., 2002; Luengen et al., 2004).

44 The advantage of 'environmental sentinel' species in ecotoxicological studies is well recognized in the scientific
45 community considering they can more reliably reflect natural ecosystem health status when compared to
46 laboratory model organisms. Bivalves are used for several decades as valuable organisms in such context
47 focused on aquatic environment considering their sedentariness, their large geographical distribution, their high
48 filtering capacity, and their ability to accumulate and concentrate contaminants in a time- and dose-dependent
49 manner (Ladeiro et al., 2017; Zuykov et al., 2013). As a result, several studies can be gathered from the literature
50 demonstrating the sensitivity of immune-relative functions of bivalve hemocytes to environmental contaminants
51 following *ex vivo*, *in vivo* and *in situ* exposures, highlighting their particular interest in the context of both
52 (eco)toxicological studies and biomonitoring surveys (e.g. Brousseau et al., 1999; Fournier et al., 2000; Luengen
53 et al., 2004; Tryphonas et al., 2005; Villela et al., 2006; Evariste et al., 2017).

54 Among bivalves, the zebra mussel *Dreissena polymorpha* has already demonstrated its relevance in such context
55 and can nowadays be considered as the counterpart of *Mytilus* species for inland waters (e.g. Binelli et al., 2014;
56 Palos Ladeiro et al., 2017). However, the use of wild species raises technical obstacles that must be unlocked, or
57 at least controlled, before their proper use in such strategies. The limited knowledge about the immune
58 physiology of some environmental species such as dreissenids (in comparison to laboratory model organisms)
59 may represent a source of confusion and a barrier for the interpretation of the biological responses following
60 exposure to contaminants. In particular, the incomplete characterization of their immune system limits the
61 understanding and the control of the variability of the responses and the cellular profiles. The open circulatory
62 system of bivalves often results in the omnipresence of undesirable material such as debris, impurities and non-
63 target exogenous or endogenous cells in *D. polymorpha* hemolymph samples that strongly impact sample quality
64 and make analyses even more complicated. There are no specific markers of *D. polymorpha* hemocytes available
65 nowadays to circumvent this difficulty. The relatively small size of adult zebra mussels (20-40 mm, in comparison

66 to *Mytilus edulis*, up to 10 cm) limits the quantity of hemolymph that can be sampled (Jones, 1983), restricting the
67 number of analyses performed and/or the experimental design (i.e. number of conditions tested per sample).
68 Additionally, the adhesion and aggregation properties of hemocytes are often ignored in experimental and
69 analytic procedures while they can be important factors to consider notably during flow analyses.

70 Here, we propose a protocol to perform the simultaneous analysis of cytotoxicity and phagocytosis activity on *D.*
71 *polymorpha* hemocytes using flow cytometry. This technic provides the advantages of being rapid and allowing
72 the immediate and quantitative acquisition of multiple morphological and functional endpoints on single cells.
73 Flow cytometric analyses already proved to be a performant tool successfully applied to the study of bivalve
74 immune system following *in vivo* or *ex vivo* exposures as well as in a physiological context (Goedken and De
75 Guise, 2004; Le Foll et al., 2010; Rioult et al., 2014; Evariste et al., 2016, 2017, 2018). The present study focuses
76 on several practical improvements in hemocyte suspension preparation and cytometric analysis (labeling and
77 gating strategy) to overcome the above-mentioned technical barriers. The main objective is to result in an
78 optimized protocol that can be routinely used for *ex vivo* exposure (i.e. chemical or environmental sample testing)
79 with a possible adaptation to *in vivo* experiments (in the laboratory or in the field). The enhancements of the
80 protocol focus on (i) the sample quality improvement, (ii) the optimization of the analyses performed regarding the
81 quantity of available biological material, (iii) a better control of inter-sample variability (in terms of biological
82 response and cellular profiles), and (iv) the proper consideration of the adhesion/detachment of hemocytes within
83 the experimental procedures.

84

85 2 Materials and Methods

86

87 2.1 *Mussel origin and hemolymph collection*

88 Zebra mussels (1.8–2.5 cm length) were collected at the Lac du Der (Marne, France) between March and May
89 2016, and kept at least two weeks for acclimation in the laboratory before use. Mussels were maintained in
90 aerated 30 L-tanks (250-300 indiv./tank) filled with 4.5 L of natural spring water (spring Aurèle, Cristalline) and
91 equipped with a filtration system (TC-200, Aquatlantis). Water was 100 %-renewed weekly. Organisms were kept
92 at 14 ± 1 °C in the dark and fed twice a week with fresh algae (*Chorella vulgaris* and *Scenedesmus obliquus*;
93 50:50) to reach a total feed supply rate of 2×10^6 cell.indiv⁻¹.j⁻¹.

94 Hemolymph was withdrawn from mussel posterior muscle using 0.3 mL-insulin syringes fitted with 29G \times 1/2"
95 needles (Myjector®, Terumo®). Syringes were rinsed using modified Leibovitz's L15-medium (L15-15%⊕: 15%
96 (v/v) L15 medium, 85% (v/v) distilled water, phenol red 0.03 mM, 10 mM HEPES, 2 mM L-Glutamine, 0.1 mg.mL⁻¹
97 Streptomycin, 100 U.mL⁻¹ Penicillin, pH 7.5, 0.2 μ m-filtered; Evariste et al. (Evariste et al., 2016)) and filled with
98 50 μ L of medium before hemolymph sampling. Hemolymph samples can be individual or pooled samples from
99 four or five mussels. Samples were then stored in sterile microtubes in a rack previously placed on ice. Cell count
100 was performed on each sample using KOVA® Glasstic® slides with grids (Hycor Biomedical) according to the
101 manufacturer's recommendations.

102 For the comparison of the results between pooled and individual samples, four individual samples of total
103 hemolymph (i.e. hemocytes and plasma) were used to constitute a pooled sample. The adequate volume
104 representing a quarter of the total number of cells needed (i.e. 50×10^3 cell.well⁻¹, for instance) of each individual
105 sample was added to the pooled sample.

106

107 2.2 *Hemocyte ex vivo exposure*

108 Immediately after cell count, 50, 75 or 100×10^3 cell.well⁻¹ were deposited in a 96-well microplate (U-bottom
109 CellStar® 96 Well Culture Plate, Greiner Bio-One). Each volume was completed to 300 μ L with L15-15%⊕
110 medium (or to 290 μ L plus 10 μ L of contamination solution for an exposure condition). 2.0- μ m diameter yellow-
111 green (YG) fluorescent polystyrene microspheres (Fluoresbrite® carboxylate microspheres, PolyScience) were
112 also added with a 1:50 hemocytes-beads ratio to measure the phagocytic activity of hemocytes. Samples were
113 conscientiously homogenized and then incubated for 4 h at 16 °C. Hemocyte mortality was then evaluated using
114 propidium iodide (PI) solution (1.0 mg.mL⁻¹; Sigma-Aldrich) added at 1% (v/v final) just before cytometric analysis
115 (Evariste et al., 2016, 2017).

116

117 2.3 Protocol optimized steps

118 2.3.1 Sedimentation step

119 To enhance the quality of the hemocyte deposit, a sedimentation step was realized as follows. Just after
120 hemolymph deposition in a 96-well microplate, samples were kept for 20 min at 16 °C to allow the hemocytes to
121 settle and adhere to the substrate (*i.e.* the bottom of the microplate well). The supernatant was removed and
122 190 µL of L15-15%[⊕] medium were added. Then, the protocol continued as previously described in *part* 2.2.

123

124 2.3.2 Cell detachment step

125 A trypsin treatment was used to re-suspend hemocytes adherent to the microplate substrate at the end of the
126 exposure period. Thus, 10 min (or 15 min when the cellular probe is used) before the end of the incubation
127 period, each supernatant was transferred to a new 96-well microplate dedicated to cytometric analysis. Then,
128 100 µl of Trypsin-EDTA solution (Trypsin-EDTA 1 × solution purchased from Sigma-Aldrich and 4-fold diluted in
129 0.20-µm filtered demineralized water) were added in each emptied well used for cell exposure. After 10 min of
130 incubation at room temperature, samples were thoroughly homogenized and transferred in the new microplate to
131 obtain a total volume of 300 µL per sample containing both freshly detached hemocytes and supernatant.
132 Afterward, dyes (PI and/or Hoechst) were added as described in *parts* 2.2 and 2.3.3.

133

134 2.3.3 Cellular probe

135 Hoechst[®] 33342 (Trihydrochloride trihydrate, ThermoFisher Scientific) is a nucleic acid stain commonly used as a
136 vital cell-permanent nuclear counterstain emitting blue fluorescence when bound to double-strain DNA. The
137 staining was performed on hemolymph samples adding 1% (*v/v* final) of Hoechst 500 µM solution (obtained from
138 successive dilutions of the 20 mM-commercial solution in 0.20-µm filtered demineralized water) followed by 10
139 minutes of incubation at room temperature. This step was carried out just before PI addition before sample
140 analysis and resulted in a triple-labeling (PI, YG beads and Hoechst) of the samples.

141

142 2.4 Flow cytometric analysis

143 Cytometric analyses were performed using Accuri[™] C6 flow cytometer (Becton Dickinson) equipped with blue
144 473 nm- (on FL1 and FL3 channels) and UV 375 nm-lasers (on FL2 and FL4 channels). BD Accuri[™] C6 software
145 (v1.0.264.21) was used to analyze the data files. The hemocyte region (R1) was identified using cellular
146 morphological parameters: forward scatter (FSC-A) for particle size and side scatter (SSC-A) for internal

147 complexity (Evariste et al., 2016). This region was deliberately chosen as wide enough to allow morphological
148 modifications in the hemocyte cell population in particular due to phagocytic activity. Cellular events (H+) were
149 identified using Hoechst® 33342 fluorescence recorded in the FL2 channel (427/10 nm filter). Hemocyte mortality
150 (%PI+) was evaluated using PI fluorescence analyzed in the FL4 channel through a 670 LP-filter. Phagocytic
151 parameters were determined using YG bead fluorescence in the FL1 channel equipped with a 530/30 nm filter
152 90% attenuated. The percentage of total phagocytic cells (%1B+) was defined as the percentage of hemocytes
153 that engulfed one or more bead(s). The percentage of cells that engulfed three or more beads represented the
154 percentage of efficient phagocytic cells (%3B+). The mean number of efficiently engulfed beads per cell was
155 calculated by dividing the mean FL1 fluorescence relative to three or more beads by the mean FL1 fluorescence
156 of one bead (Evariste et al., 2017). Each sample was analyzed for 10^4 events (or Hoechst-positive [H+] events
157 when the cellular probe is used) in the R1 region at a flow rate of $66 \mu\text{L}\cdot\text{min}^{-1}$. To ensure the validity of data
158 comparison between samples and tests during protocol optimization and validation, the fluorescence thresholds
159 used for the analysis of each dye were defined superposing the fluorescence profiles of all the samples from the
160 same test and kept similar for subsequent series of tests as far as possible.

161

162 2.5 Statistical analysis

163 Statistical analyses were conducted using Statistica 8.0 software (Statsoft, Inc.). The statistical procedure
164 depended on the experimental design performed and the nature of the dataset. First, results were systematically
165 tested for residual normality using Shapiro-Wilk's test with a 1%-risk.

166 For independent samples, homoscedasticity was tested with Brown-Forsythe's test (5% risk). The datasets which
167 fulfill normality and homoscedasticity criteria were then analyzed with a one-way or two-way ANOVA followed by
168 a posthoc Tukey's test ($\alpha = 0.05$). Otherwise, the Mann-Whitney U test ($\alpha = 0.05$) was used as a non-parametric
169 alternative for two independent samples analysis.

170 For dependent samples, a *t*-test for dependent samples was performed to compare two samples showing normal
171 distribution. When more than two groups were compared, repeated-measures ANOVA followed by posthoc
172 Tukey's test was performed ($\alpha = 0.05$). Sphericity assumption was previously checked using the Mauchly test
173 ($\alpha = 0.05$). For the comparison of two samples showing non-normal distribution, the Wilcoxon matched-pairs test
174 ($\alpha = 0.05$) was performed.

175 **3 Results and Discussion**

176

177 *3.1 Pool versus individual samples*

178 One of the first obstacles that could be encountered working on *D. polymorpha* hemocytes is the quantity of
179 biological material available per individual (from 1 to 3×10^5 cells per sample, or about 4 deposits of 75×10^3 cells
180 at most). This can strongly limit the analysis performed on each sample and the number of tested conditions
181 during *ex vivo* experiments. A simple way to solve these issues consists of pooling hemolymph samples from
182 several individuals (e.g. Auffret and Oubella, 1997; Hégaret et al., 2003; Labreuche et al., 2006; Hinzmann et al.,
183 2013; Tanguy et al., 2013). Besides it allows more flexibility in the experimental design particularly for *ex vivo*
184 experiments, cellular profiles (SSC-FSC profiles) of pooled samples proved to be less variable than individual
185 ones (Figure 1). The latter samples often exhibit several subpopulations of hemocytes that could be hardly
186 identified as their shape and the position on the SSC-FSC profile could strongly vary (Figure 1A). These
187 variations in hemocyte scattering profiles could generate an overlap with other endogenous (e.g. gill cells) or
188 exogenous (e.g. microorganisms, algae) cells. Moreover, some cellular activities such as phagocytosis result in
189 considerable disturbances of scattering parameters that prevent from identifying hemocyte subpopulations
190 (Evariste et al., 2017). Cell mortality could also lead to morphological modifications which could be wrongly
191 interpreted as a hemocyte sub-population (Figure 2), particularly when mortality is not simultaneously assessed.
192 In the example proposed in Figure 2, cell mortality can be evaluated at 1.4% or 45.5% if the analyze focuses on
193 P2- or P3-population, respectively. These values are both far from the average mortality of 24.7% evaluated in
194 the global hemocyte region (R1). All these aspects could lead to variation in analyzed biological endpoints and/or
195 skewed result interpretation considering that hemocyte functionalities are also significantly varying and are
196 differentially modulated following chemical exposure according to the hemocyte subtype (Evariste et al., 2016,
197 2017). As a result, pooled samples could represent a valuable alternative in experiments where inter-individual
198 variability may mask toxic responses following exposure dedicated to chemical or environmental samples toxicity
199 assessment. For instance, the variability of the percentage of PI-positive events (%PI+) in the hemocyte region,
200 evaluated with the coefficient of variation (CV), was shown to reach 53% in individual samples (N = 16) whereas
201 a value of 26% was observed for pooled samples (N = 4) made from these individual samples (Supplemental
202 Information Figure S1A). The use of pooled samples of hemolymph thus ensures that several conditions (e.g.
203 different compounds or concentrations) could be tested with the same sample while increasing the power of
204 discrimination between responses from various exposure conditions by limiting inter-sample variability. The major
205 challenge of toxicity testing procedures is the global toxicity assessment of target substances, mixtures or
206 effluents. Thus, the use of pooled samples in such an approach may not be a hindrance as it gives information on
207 the toxic impact on the overall hemocyte population. In such kind of study, the differential toxicity among
208 hemocyte subpopulations may represent a weaker interest in comparison to the improvement of an experimental
209 design in which several compounds/concentrations can be tested on the same sample (thus allowing the

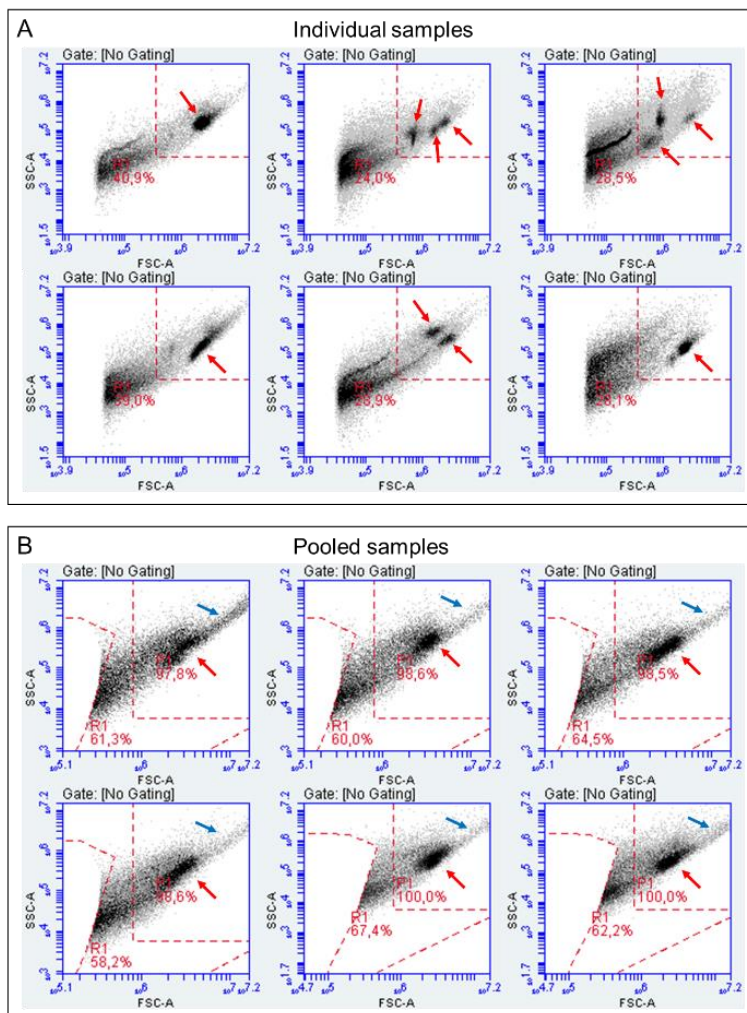
210 comparison of the toxicity among treatments). Hégaret et al. (2003) already validated the use of pools of
211 hemolymph (instead of individual samples) to evaluate cell mortality and phagocytosis in oysters *Crassostrea*
212 *virginica*. Individual samples are nonetheless of great interest in field and/or physiological studies where inter-
213 individual variations and/or sub-population differential responses remained highly informative.

214 It must be noticed that the %PI+ observed in pooled samples is systematically (even insignificantly) higher than
215 the mean value calculated from the corresponding individual samples (*Figure S1B*). This increase in cell mortality
216 is concomitant with the non-negligible formation of cellular clumps (or small aggregates) which could be observed
217 on the right upper part of the scatter profiles (*Figure 1B*). Cell-to-cell interactions and aggregate formation have
218 been reported in hemocytes from various bivalve species including marine mussels and oysters. Hemocyte
219 aggregation is known to be a spontaneous event occurring within minutes after removal of hemolymph from
220 bivalve mollusks (Auffret and Oubella, 1997; Chen and Bayne, 1995; Le Foll et al., 2010). Le Foll et al. (Le Foll et
221 al., 2010) demonstrated by time-lapse video microscopy that basophil hemocytes in *Mytilus edulis* species were
222 involved in dynamic hemocyte-hemocyte interactions and the constitution of aggregate cores. Basophil (or Blast-
223 like) cells have also been identified in *D. polymorpha* and share similar morphometric characteristics (Evariste et
224 al., 2016). This may explain the systematic disappearing of this hemocyte sub-population characterized by small
225 size (FSC) and low internal complexity (SSC) in pooled samples as shown on scatter profiles (*Figure 1B*).
226 However, it must be emphasized that the classification of hemocyte subpopulations in bivalves remains largely
227 controversial, impeded by a lack of consensus due to the use of different parameters and techniques to define
228 their classification (Le Foll et al., 2010; Rebelo et al., 2013). The work of Rebelo et al. (Rebelo et al., 2013)
229 supported the theory that the different subpopulations of hemocytes in the oyster *Crassostrea rhizophorea* are in
230 fact different stages of one type of cells from immature cells (Blast-like or basophil cells) which, when mature,
231 accumulates granules (granulocytes) or degranulates (hyalinocytes) in the event of environmental stress. In the
232 present study, the main hemocyte population observed in pooled samples (*Figure 1B*) corresponds to
233 'hyalinocyte' sub-population. This can suggest that mixing hemolymph samples from different individuals
234 generates mature hemocyte degranulation leading to one single population of agranular hemocytes. These
235 overall observations could be interpreted as the first signs of some allorecognition in *D. polymorpha* hemocytes.
236 However, further studies are needed to confirm such a hypothesis as allorecognition in bivalve has not been
237 clearly reported nowadays (Costa et al., 2009). If confirmed, such phenomenon could also explain the slight
238 increase of cell mortality observed in pooled samples when compared to individual ones.

239 Similarly, results showed that cell mortality significantly increased with the number of deposited cells (from 50×10^3
240 to 100×10^3 , *Figure S2*) with a concomitant increase of value heterogeneity. These observations drew attention to
241 the importance of keeping cell number identical to prevent skewing data interpretation, particularly in comparative
242 studies such as chemical toxicity assessment. As a good compromise between cell mortality, data variability and
243 the requirement to analyze 10,000 events (or H+ events) in the hemocyte region, we chose to deposit 75×10^3

244 cells per well in subsequent experiments. This size of deposit ensures an experimental design adapted to test at
245 least 8 conditions on the same sample and up to 15 conditions on average (median value, N = 47).

246

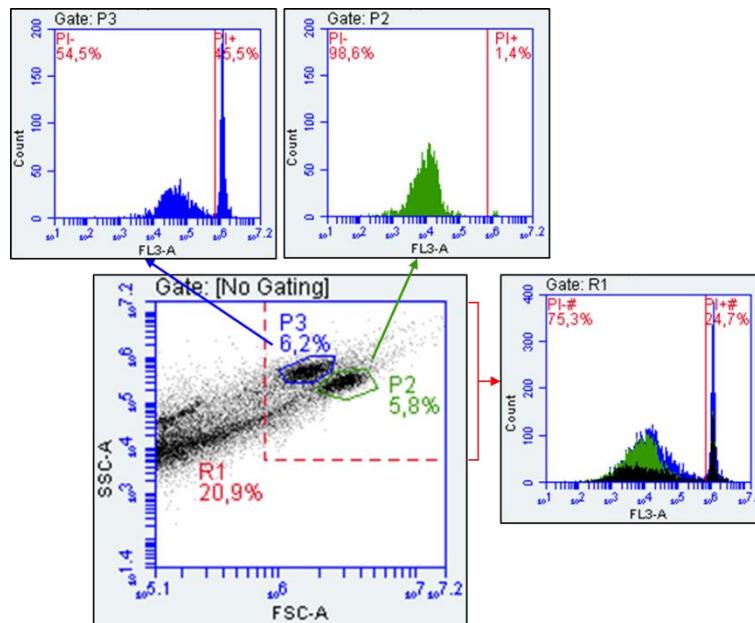


247

248

249 **Figure 1.** Examples of cellular profiles (SSC-FSC; raw data voluntarily presented) of fresh individual (A) and
250 pooled (B) samples (N = 5) of *Dreissena polymorpha* hemolymph analyzed by flow cytometry. Red and blue
251 arrows point out cellular (sub)-populations and cellular clumps, respectively.

252



253

254 **Figure 2.** Cell mortality (i.e. the percentage of PI+ events) measured in which prima facie could be considered as
 255 different hemocyte subpopulations from fresh individual samples of hemolymph (raw data voluntarily presented).
 256 The P2 and P3 regions surround two hemocyte subpopulations whereas the R1 region delimits the global
 257 hemocyte region.

258

259 3.2 Protocol pre-analytical phase optimization

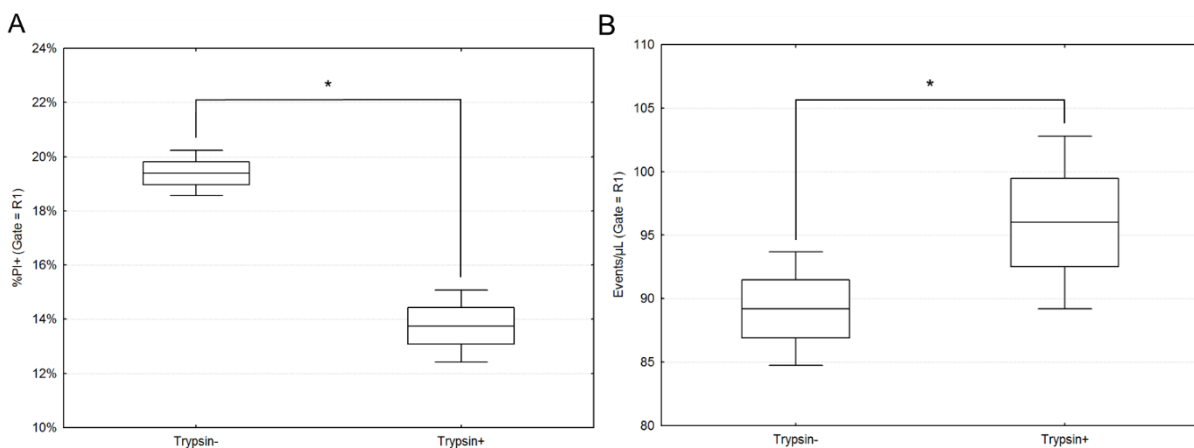
260

261 3.2.1 Cell detachment using Trypsin-EDTA: collecting the 'forgotten' cells

262 Hemocytes are circulating cells capable of fast tissue infiltration and strong adhesion to foreign surfaces. Cell
 263 sedimentation and adhesion to the substrate are systematically observed after hemolymph withdrawal, reflecting
 264 hemocyte activation (Riout et al., 2013). This property is indubitably problematic when the analytical technics
 265 required that the cells remained isolated and in suspension such as for flow cytometry measurements. This
 266 aspect is unfortunately regularly neglected in studies analyzing bivalve hemocytes by flow cytometry (e.g. Sauv e
 267 et al., 2002; Labreuche et al., 2006; Tanguy et al., 2013; Le Guernic et al., 2015; Evariste et al., 2016, 2017,
 268 2018). After the addition of a cell detachment step just before cytometric analyses using diluted Trypsin-EDTA
 269 solution, results showed that the %PI+ events detected in the R1 region are significantly lower (Figure 3A). The
 270 decrease in the %PI+ is concomitant to a significant increase in the event rate detected by the cytometer in the
 271 R1 region (Figure 3B), confirming that the trypsin treatment successfully detached adherent cells from the
 272 microplate wells. The increase in the number of adherent (and thus viable) cells in the acquisition gate resulted in
 273 an 'artefactual' diminution of the %PI+ in comparison to untreated samples. These results demonstrate that the
 274 %PI+ is significantly over-estimated in untreated samples where a non-negligible number of viable cells remains
 275 stick onto the plastic substrate. It proves the importance of accounting for the hemocyte adhesion ability during
 276 the preparation of the samples dedicated to flow cytometric analysis, otherwise the results may not be

277 representative of the whole hemocyte population present in the microplate well. It could be particularly true in
 278 functional analysis such as phagocytosis activity, considering that adhesion constitutes an initial step of
 279 phagocytosis process (Labreuche et al., 2006; Tanguy et al., 2013). In the literature, several
 280 antiaggregant/adhesive solutions are used during bivalve hemolymph preparation including heparin, EDTA,
 281 (modified) Alsever's solution, N-ethylmaleimide and calcium-free trypsin-EDTA (Grandiosa et al., 2016, 2018;
 282 Hégaret et al., 2003; Hinzmann et al., 2013; Huang et al., 2018; Le Foll et al., 2010; Rebelo et al., 2013). Both
 283 heparin and low temperature have been reported as ineffective in preventing invertebrate hemocyte aggregation
 284 (Grandiosa et al., 2018; Hinzmann et al., 2013). (Modified) Alsever's and EDTA solutions proved to be a suitable
 285 treatment in marine bivalves such as abalones, blue mussels or oysters (Grandiosa et al., 2016, 2018; Hégaret et
 286 al., 2003; Le Foll et al., 2010; Rebelo et al., 2013). However, these antiaggregant solutions are not applicable in
 287 freshwater species as they impact cell morphology and viability regarding the low osmolarity of freshwater bivalve
 288 internal fluids (Hinzmann et al., 2013). In particular, hemolymph osmolarity in *D polymorpha* species was
 289 measured at around 80 mOSM (Quinn et al., 2009). In our study, the commercial trypsin-EDTA solution had to be
 290 diluted by 4 before use to prevent hyperosmolarity issues. This treatment was the most efficient method to
 291 increase the number of functional cells analyzed by flow cytometry. However, the action of trypsin is rapidly
 292 inhibited when the enzyme is diluted at the end of the step #5 (see Table 1). Samples have thus to be quickly
 293 analyzed thereafter. To limit hemocyte sedimentation and re-adhesion to the substrate, cell suspensions are
 294 regularly and thoroughly mixed by pipetting before analysis. This homogenization method has been reported as
 295 efficient to mix cell suspension while maintaining high viability rates in abalone hemocytes even if vortexing
 296 should be preferred (Grandiosa et al., 2018). This latter method could not be performed with microplates.

297



298

299 **Figure 3.** Effects of Trypsin-EDTA treatment on the cell mortality (%PI+; A) and the cell rate (number of events
 300 detected per microliter; B) in the hemocyte region (R1) analyzed by flow cytometry. Data are presented as the
 301 mean value (horizontal line) \pm SD (box). The whiskers represent the mean value \pm 1.96*SD. Asterisks mark
 302 significant differences ($p < 0.05$) with (+) or without (-) trypsin-treatment, according to Mann-Whitney U test ($N = 5$
 303 deposits from the same pool per treatment).

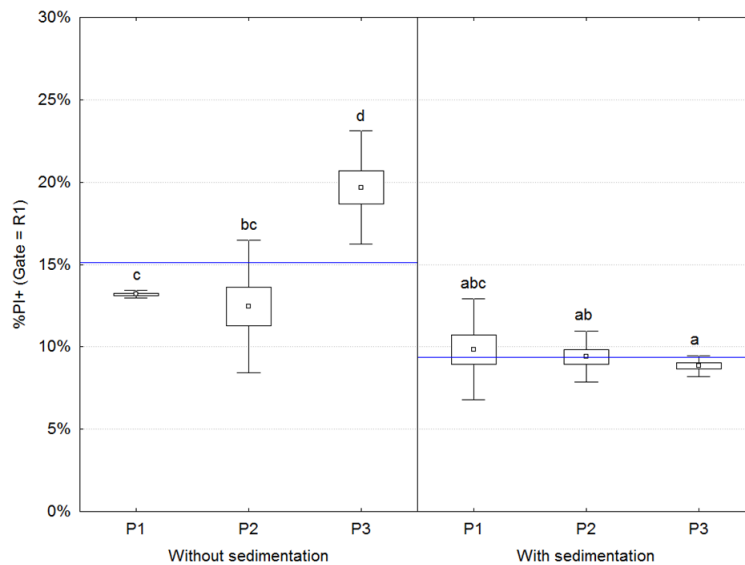
304

305 3.2.2 Functional cell selection using a sedimentation step

306 The ability of hemocytes to strongly stick to a foreign surface in the minute range was the main difficulty
307 encountered when performing flow cytometry analyses on such cell types. However, it is also possible to take
308 advantage of hemocyte adhesion ability to increase the quality of the cell suspension before *ex vivo* exposure. A
309 sedimentation step was proposed just before cell exposure, relying on the idea that a selection of functional (and
310 thus viable) hemocytes could be performed based on their adhesion-to-substrate ability. Considering that
311 adhesion constitutes an initial step in the phagocytosis process (Labreuche et al., 2006), this selection of cells
312 based on their adhesion ability may be very appropriate to further perform a functional bioassay such as
313 phagocytosis analysis.

314 Previous tests revealed that the %PI+ events in the hemocyte region were significantly higher at T0 than after 4h
315 of incubation (*Figure S3*). These observations suggested that hemolymph withdrawal may result in a cellular
316 shock that triggers cell death or at least a loss of membrane integrity. After 4h of incubation, cells may have
317 recovered resulting in lower %PI+ events, considering that the cell concentration remained stable over time ($\rho =$
318 0.1, data not shown). It seems that the hemocyte population is not in a 'stable state' and that it takes time to
319 recover from the effects generated by hemolymph withdrawal. Thanks to a sedimentation step, results showed
320 that the %PI+ was not anymore significantly different between T0 and T4 (*Figure S3*) indicating that the hemocyte
321 population status remained stable over the incubation time.

322 The *Figure 4* illustrates the effects of the sedimentation on the cell mortality for different pooled samples. A
323 Factorial ANOVA was conducted to evaluate the influence of the sample (P1 to P3) and the treatment
324 (sedimentation or not) on the %PI+ events in the R1 region. The analysis revealed that the main effects were
325 statistically significant as well as the interaction. The significant interaction between the "Sample" and the
326 "Treatment" factors ($F_{(2,12)} = 17.3$; $p < 10^{-2}$) indicated that the effect intensity of the sedimentation step on the
327 %PI+ is dependent on the considered sample. In the present case, the effect is more important in P3-sample
328 showing the highest %PI+ value without sedimentation. The sedimentation step thus provides two main
329 advantages: first, it notably reduced the cell mortality level after 4h of incubation (< 10% in the present example)
330 and secondly, it erased inter-sample variability with mean %PI+ values very similar and globally less variable in
331 comparison to what is observed without sedimentation step (*Figure 4*).



332

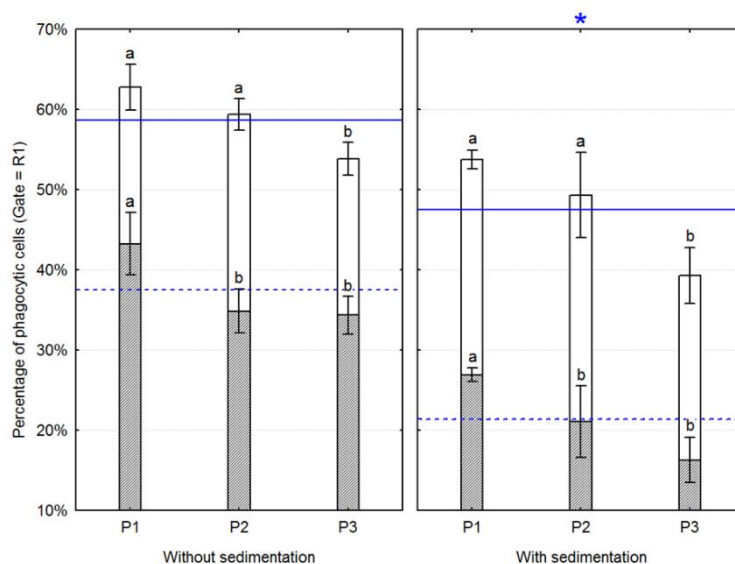
333 **Figure 4.** Effects of the sedimentation step on the percentage of PI+ events in the hemocyte region (R1)
 334 measured in three pools of hemolymph after 4h of incubation. Data are presented as mean value (empty square)
 335 \pm SE (box; N = 5). The whiskers represent the mean value \pm 2*SD. A Factorial ANOVA followed by the Tukey
 336 HSD test was conducted to analyze the effects of the sample (P1 to P3) and the treatment (with or without the
 337 sedimentation step) on the %PI+. Groups with different letters are significantly ($p < 0.05$) different from each other
 338 within the interaction effect. Blue lines indicate the mean value of each treatment group for illustrative purposes.

339 The effect of the sedimentation step was also analyzed on phagocytosis activity after 4h of incubation (Figure 5).
 340 A Factorial ANOVA was performed to analyze the effects of the sample and the sedimentation step on the
 341 percentage of the total (%1B+) and efficient (%3B+) phagocytic cells in the R1 region. This procedure gave
 342 similar results for both parameters with significant “Sample” ($F_{(2,12)} = 21.9$ with $p < 10^{-4}$ and $F_{(2,12)} = 16.2$ with
 343 $p < 10^{-3}$, respectively) and “Treatment” main effects ($F_{(2,12)} = 58.4$ with $p < 10^{-5}$ and $F_{(2,12)} = 122.8$ with $p < 10^{-6}$,
 344 respectively). The interaction effects were insignificant. The same analysis performed on the hemocyte avidity
 345 (i.e. mean number of efficiently engulfed beads per cell) proved to be insignificant and is thus not presented here.
 346 The results on the %1B+ and the %3B+ indicated that the inter-sample variability of these endpoints remained
 347 significant with or without a sedimentation step. Phagocytosis activity was lower in samples following the
 348 sedimentation and associated with a lower concentration of events detected in the R1 region in comparison to the
 349 unmodified protocol (data not shown). Hemolymphatic supernatant removal following the sedimentation step may
 350 explain these observations as many soluble humoral factors (such as pathogen recognition receptors) are
 351 present in the plasma of hemolymph (Leprêtre et al., 2019). Moreover, the beads used here have a non-specific
 352 coating with carboxylates and could thus bound to bacteria, viruses or debris which could, in turn, be recognized
 353 and stimulate phagocytosis activity of hemocytes. Their removal from the medium could hypothetically limit
 354 phagocytosis activation. As a result, the sedimentation step results in a phagocytic activity at a low or un-
 355 activated state of the cells. Further studies are needed to explore the reason for such an effect on phagocytosis
 356 measurements in *D. polymorpha* hemocytes.

357 The addition of a sedimentation step in the protocol nonetheless provides the advantage of focusing on functional
 358 cells during subsequent flow cytometry analysis while reducing cell mortality and inter-sample variability. These

359 aspects are of great interest notably for *ex vivo* exposure. The sedimentation step should however not be
 360 systematically performed in the case of *in vivo* exposure of mussels as the removal of dead and non-functional
 361 cells from the sample following sedimentation could biased results. The decision to include or not a selection of
 362 analyzed cells has to be well-considered in the light of the own objectives of the experiment.

363



364

365 **Figure 5.** Effects of the sedimentation step on the percentage of the total (white bars; %1B+) and efficient
 366 (hatched bars; %3B+) phagocytic cells in the hemocyte region (R1) measured in three pools of hemolymph after
 367 4h of incubation. Data are presented as mean value \pm SD (N = 5). The solid and dashed blue lines represent the
 368 mean group value for %1B+ and %3B+, respectively. A Factorial ANOVA was conducted to compare the main
 369 effects of the sample (P1 to P3), the treatment (with or without the sedimentation step) and the resulting
 370 interaction on the %1B+ and %3B+. Tukey HSD test was used as a posthoc test. Samples with different letters
 371 are significantly ($p < 0.05$) different from each other within the sample main effect. The blue asterisk illustrates the
 372 significant difference within the treatment main effect ($p < 10^{-3}$).

373

374 3.3 Multi-labeling analysis in flow cytometry

375 The open circulatory system of bivalves and the omnipresence of debris and of (exo- or endogenous) non-target
 376 cells in *D. polymorpha* hemolymph strongly impact sample quality. The adequate positioning of the gate of
 377 interest (R1) helps to eliminate the main part of these undesirable events during the post-acquisition treatment of
 378 flow cytometry data. The addition of a cellular probe can nonetheless refine the results of hemocyte analysis by
 379 discriminating nucleated events from debris in the hemocyte region. Hoechst® 33342 was selected as non-
 380 specific nuclear counterstain considering that (i) no specific dye are available for *D. polymorpha* hemocytes
 381 nowadays, and (ii) its great cell-permeability allowing a short staining time. Hoechst® 33342 is excitable by an
 382 ultraviolet laser and emits a strong blue fluorescence making it compatible in a multi-labeling procedure using PI
 383 and YG beads (see discussion below). The combination of these three dyes resulted in a complete cytometric
 384 analysis focused on cellular (Hoechst-positive; H+) events in the hemocyte region with a simultaneous

385 assessment of cytotoxicity (PI staining) and phagocytic activity (YG beads), as illustrated in *Figure 6*. The main
386 challenge in the choice of the trio of dyes relies on the compatibility of the cellular and mortality probes regarding
387 the wide emission spectrum of YG beads. The trio of dyes was first selected according to their excitation/emission
388 spectrum provided by the suppliers and the laser configuration of our cytometers. The dyes were then tested
389 individually, by pairs and finally the trio Hoechst/PI/beads, on five pooled samples during a single experiment.
390 The fluorescence profiles of each combination of probes were analyzed in comparison of the profile of the dye
391 alone to evaluate the modification of the fluorescence profiles in the presence of several dyes.

392 For the probes alone, the most variable profiles were observed for Hoechst labeling (*Figure S4A*) sometimes
393 requiring an adaptation of H+ fluorescence threshold for some samples or batch of samples. The addition of
394 beads resulted in a slight increase of H+ fluorescence profile variability (*Figure S4C and D*) whereas no effect of
395 PI was visible (*Figure S4B*). Nonetheless, no significant difference was shown in the %H+ events in the R1 region
396 for the different combinations of probes ($p > 0.05$ according to repeated-measures ANOVA; data not shown). The
397 PI fluorescence profiles were very similar among samples for the probe alone (*Figure S5*). The addition of the
398 Hoechst probe increased PI fluorescence intensity as shown by a rightward shift of the whole PI profile (i.e. cell
399 autofluorescence and PI+ peak; *Figure S5B*). This is probably the result of a slight overlap between Hoechst and
400 PI fluorescence profiles (Hoechst[®] 33342 dye also emits in red wavelengths). The double-labeling using PI and
401 beads also changed the FL4-fluorescence profile but only by increasing the cell autofluorescence resulting in a
402 slight overlap of PI+ fluorescence peak (*Figure S5C*). The triple-labeling procedure resulted in a combination of
403 these effects on PI fluorescence: an increase of cell autofluorescence and a rightward shift of the PI+ profile
404 (*Figure S5C*). The PI+ fluorescence thresholds had thus to be adapted to coherently analyze PI labeling in triple-
405 or double- (H+PI) labeled samples. With such adaptations, the percentage of PI+ cells in the R1 region did not
406 significantly differ ($p > 0.05$ according to repeated-measures ANOVA) among the different labeling conditions (PI
407 alone, PI+H, PI+B, and PI+H+B). No effect of PI or Hoechst was observed on the bead fluorescence profile
408 whatever the conditions (*Figure S6*). Accordingly, no statistical differences between labeling conditions were
409 highlighted on phagocytosis endpoints (i.e. %1B+, %3B+, and avidity) in the R1 region ($p > 0.05$ according to
410 repeated-measures ANOVA; data not shown).

411 These results demonstrate the compatibility of the three selected probes for the simultaneous analysis of
412 cytotoxicity and immunotoxicity in *D. polymorpha* hemocytes. PI and Hoechst[®] 33342 have been already used in
413 a double-labeling procedure on hemocytes from silkworms and nematodes (Li et al., 2009; Okazaki et al., 2006).
414 To our knowledge, this is the first time that a functional triple-labeling procedure is proposed for bivalve
415 hemocytes. PI probe is classically excited in blue wavelength (at 480 nm) but it is also possible to excite it with a
416 UV laser to limit the potential overlap with the broad YG bead excitation spectrum. Despite a partial overlap
417 between Hoechst and PI emission spectrum, an adjustment of PI+ threshold eliminated the influence of Hoechst
418 on the analysis of PI+ cells. The use of a cellular probe as the Hoechst[®] 33342 dye provides the substantial
419 advantage of bypassing the problematic of the presence of untargeted events (i.e. debris etc.) in hemolymph
420 samples. Focusing on H+ events eliminates the non-nucleated (H-) events from the analysis as well as algal cells

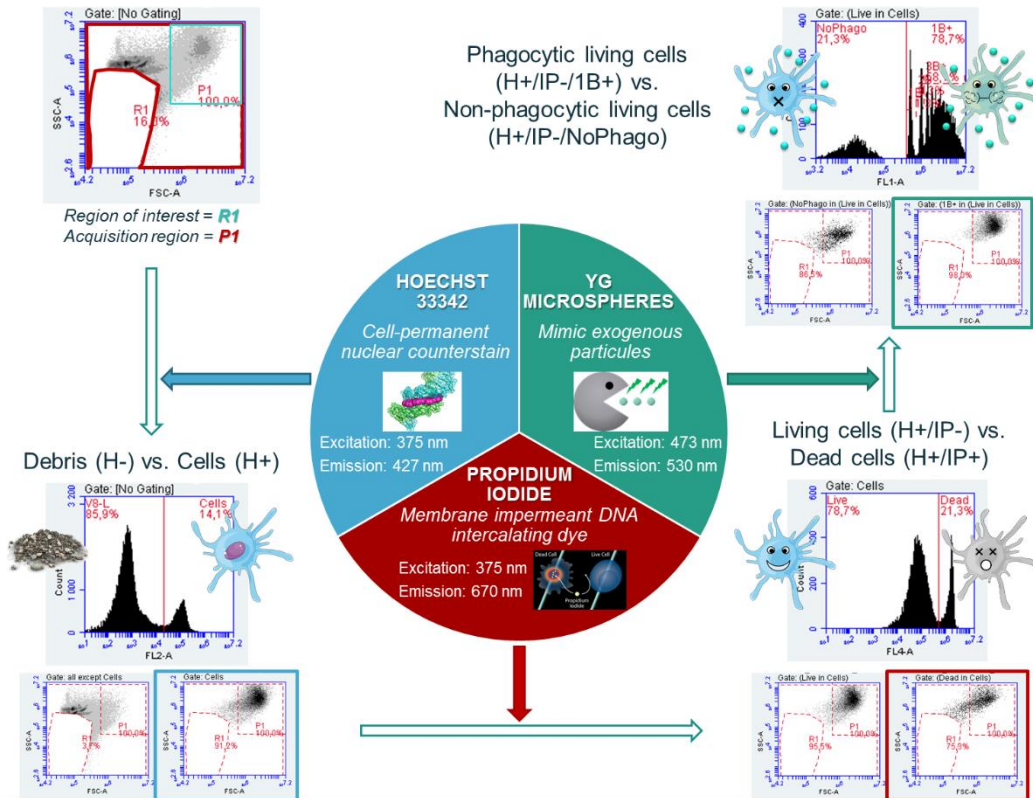
421 as *Chlorella vulgaris* (used to feed mussels) which did not integrate this dye whereas their FSC-SSC profile can
422 partially overlap the R1 region (data not shown). Despite spermatozooids are generally observed out of the R1
423 region due to their lower size and complexity in comparison to hemocytes, the addition of Hoechst allows their
424 discrimination from the cells of interest by the linear analysis of Hoechst emission profile to differentiate cell DNA
425 content ($1n$ versus $2n$). The best gating strategy is to focus on H⁺ events in the R1 region to tighten the data
426 analysis on the hemocyte cell population. Even with an acquisition region eliminating the most part of the debris
427 and small-sized events (e.g. the P1 region; see *Figure 6*), the percentage of H⁺ events only represents 45% of
428 the total events on average (N = 12 pooled samples) with values ranging from 15% for the 'dirtiest' to 58% for the
429 'cleanest' sample. In the R1 region, the percentage of H⁺ events is much higher, with an average value equal to
430 $77\% \pm 4.2\%$, indicating that cells are the main part of the detected events and thus validating the position of this
431 region of interest on the FSC-SSC profile. It nonetheless also highlighted that more than 20% of the events
432 detected in this region are not cells and may thus bias the endpoint acquisition if no cellular probe is used. In the
433 absence of specific labeling of *Dreissena* hemocytes, the use of Hoechst dye enhances the quality of the
434 cytometric analysis in such an organism for which the presence of debris in hemolymph samples is inevitable.

435 Besides the triple-labeling procedure reduces the quantity of biological material needed and allows the
436 simultaneous analysis of cytotoxicity and immunotoxicity on the same sample, it also permits to have more
437 complete and accurate measurements of the recorded biological endpoints. For instance, in our experiments, the
438 mean %PI⁺ was equal to 16% when acquired in the R1 region as classically done, whereas it raised around 21%
439 on average when analyzed in the cells (H⁺ events) in R1 (*Figure 7A*). Without this cellular probe, the hemocyte
440 mortality could thus be underestimated by 5% on average. Similarly, the %PI⁺ is significantly higher when
441 evaluated in overall cells without R1 gating in comparison with cells in R1 gating (*Figure 7A*). The mortality is thus
442 overestimated of 3.6% on average when the population of analyzed cells is not restricted according to their FSC-
443 SSC profile. More important differences were highlighted on the phagocytosis endpoints according to the gate of
444 analysis (*Figure 7B*). In particular, the percentage of the total (%1B⁺) and efficient (%3B⁺) phagocytic cells were
445 significantly 10%-higher on average when analyzed in cells in R1 (H⁺ in R1) when compared to acquisition on the
446 R1 region, as classically done. An advantage of the triple-labeling procedure relies on the possibility to evaluate
447 phagocytosis endpoints on viable cells (H⁺/IP⁻) only. Phagocytosis analysis can be done with no direct impact of
448 potential cytotoxicity on the recorded data. In our example, %1B⁺ and %3B⁺ were more than 15%
449 underestimated on average ($p < 0.05$) when classically analyzed in the R1 region in comparison with a focused
450 analysis on viable cells in the same region (*Figure 7B*). Interestingly, the hemocyte avidity did not show any
451 significant variation according to the gate of analysis, demonstrating that this endpoint is very robust whatever the
452 gating strategy. Nonetheless, we recommend using a focused gating strategy on the viable cells present in the
453 R1 region to assess the ability and the efficiency of the phagocytosis process in hemocyte without any impact of
454 cell mortality on the generated data. It may be of great interest during chemical toxicity testing where acute
455 cytotoxicity may occur and artefactually decrease the percentage of phagocytic cells. The comparison between
456 the %PI⁺ acquired in the cells in R1 and in phagocytic (1B⁺) cells in R1 could inform on potential cytotoxicity

457 generated by phagocytosis activity during the incubation period. In our example, the mean %PI+ in cells in R1
458 was 22.2% whereas it was equal to 16.7% in phagocytic cells in R1 showing that no particular cytotoxicity was
459 induced by phagocytosis activity. Finally, the analysis of the percentage of viable cells with no phagocytic activity
460 (%1B- in viable cells in R1) can potentially highlight the presence of a phagocytosis inhibitor in the exposure
461 medium.

462 The triple-labeling procedure presented here notably enhances the representativity of the generated data through
463 the better discrimination between targeted and untargeted events. It also allows for the acquisition of additional
464 data to describe more precisely the cytotoxicity and the immunotoxicity of the tested conditions by using an
465 adequate post-gating strategy. The proposed trio of dyes required a cytometer equipped with an UV-laser to be
466 functional and this may be a limiting factor considering that this feature is not very frequent in cytometer with a
467 classic configuration. Works are in progress in our laboratory to propose another functional trio of probes with no
468 need for such a specific feature. In view of current knowledge, it is nowadays impossible to propose a specific
469 marker hemocyte cells. A recent study decrypted the proteome of *D. polymorpha* hemocytes using a
470 proteogenomic approach (Leprêtre et al., 2019) which could be a first step towards the identification of such a
471 specific probe but further studies are needed to achieve this objective. While awaiting the results of these
472 researches, the use of a non-specific cellular probe such as Hoechst is recommended. A double-labeling
473 procedure using PI and YG beads could nonetheless be performed on cytometers with a more classical laser
474 configuration. The absence of a cellular probe induces some bias in the generated data as demonstrated in the
475 present study, and this must be kept in mind when interpreting the results of such analysis. Indeed, each endpoint
476 may include a slight inaccuracy in the value generated which may be considered in studies evaluating the
477 physiological state of organisms, for instance. The double-labeling strategy remains valid in studies with a
478 comparative objective (e.g. comparison of the toxicity of chemicals, etc.). PI was selected as a global probe for
479 cytotoxicity assessment considering that it stains necrotic and late apoptotic cells (Sawai and Domae, 2011;
480 Wallberg et al., 2016). But the developed protocol can also be easily applied to a more detailed analysis of cell
481 mortality by combining PI measurement and caspase 3/7 analysis, as shown in a recent work from our laboratory
482 (Le Guemic et al., 2019). The present study also demonstrated that the hemocyte avidity is a very interesting
483 endpoint to record as it proved to be unaffected by protocol modifications or multi-labeling procedure.

484



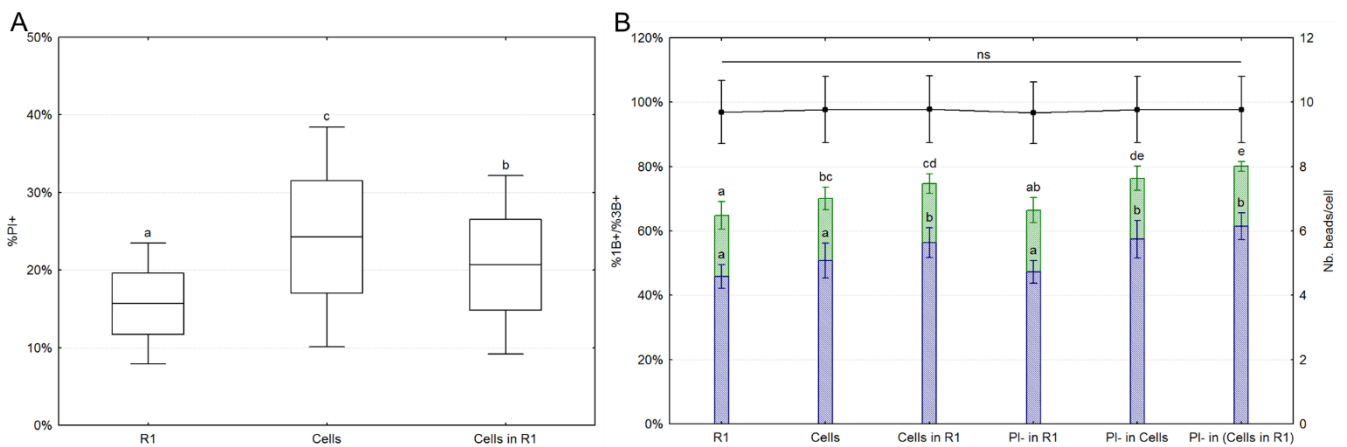
485

486

487

488

Figure 6. The principle of the triple-labeling procedure proposed for *D. polymorpha* hemocyte analysis by flow cytometry and the associated gating strategy.



489

490

491

492

493

494

495

496

497

498

499

Figure 7. Effects of the gating strategy on the mortality (%PI+; A) and phagocytosis endpoints (B). For mortality, data are presented as mean value (horizontal line) \pm SD (box). The whiskers represent the mean value \pm 1.96*SD. A repeated-measures ANOVA was performed to evaluate the effect of the gating strategy (R1, cells (H+) and cells in R1) and the treatment (PI+H and PI+H+B, N = 5 in each treatment) on the %PI+ events. No significant effect was observed for the treatment effect and the interaction Gate*Treatment ($p > 0.05$). Results are thus only presented for the significant main effect "Gate" ($p < 10^{-5}$; N = 10). Different letters indicate significant differences between gating strategies ($p < 0.05$ according to Tukey posthoc test). For phagocytosis endpoints, data are presented as mean value \pm SD. The percentage of the total (%1B+) and efficient %3B+) phagocytic cells are represented by the green hatched (to the right) and the blue hatched (to the left) bars (left axis). The hemocyte avidity is represented by the black line at the top of the graph (right axis). Different letters indicate

500 *significant differences between gating strategies ($p < 0.05$ according to Tuckey posthoc test following the*
501 *repeated-measures ANOVA).*

502

503

504 **4 Conclusion**

505 The present study was dedicated to the development of a new protocol to simultaneously analyze the cytotoxic
506 and immunotoxic responses in *D. polymorpha* hemocytes using flow cytometry. To this end, some enhancements
507 were proposed to solve the following issues: the quality and the quantity of hemolymph samples, the inter-sample
508 variability of the responses and the cellular profiles, and the adhesion ability of hemocytes. The inclusion of
509 several technical improvements gives rise to an optimized version of the hemocyte exposure protocol which is
510 summarized in *Table 1*.

511 The use of pooled hemolymph samples ensures that several conditions (different compounds or concentrations)
512 could be tested with the same sample allowing the deployment of relevant experimental design, in particular for
513 *ex vivo* experiments dedicated to the evaluation of chemical or environmental sample toxicity. Simultaneously, the
514 variability of the cellular profile and of the biological endpoints was reduced, increasing the inter-treatment
515 discrimination potency of the bioassay. The consideration of the adhesion ability of hemocyte leads us to include
516 an enzymatic detachment step followed by a proper homogenization of the cell suspension just before their
517 analysis by flow cytometry to ensure that all the cells of interest (i.e. the functional cells with adhesion ability)
518 were measured. It resulted in a decrease in the cell mortality associated with an increase in the concentration of
519 analyzed events confirming that, without a cell detachment step, not all the hemocyte population is analyzed. The
520 adhesion ability of hemocyte was also proposed to select the functional hemocytes for an *ex vivo* exposure
521 followed by a functional analysis such as phagocytosis measurements. This step enhanced the sample quality by
522 reducing the cell mortality after 4h of exposure as well as the inter-sample variability. It also ensures that only
523 hemocyte potentially able to perform phagocytosis are present at the beginning of the exposure and that no non-
524 functional cells initially present in the sample will biased phagocytosis analysis. However, the sedimentation step
525 results in a selection of the analyzed cells that has to be deeply considered regarding the study objectives,
526 particularly for *in vivo* experiments where such selection of the analyzed events may constitute an important bias.
527 Finally, a triple-labeling procedure was proposed to include a cellular probe during cytometric data analysis and to
528 simultaneously analyze cytotoxicity and immunotoxicity endpoints in the same sample. In the absence of a
529 specific hemocyte probe, this labeling procedure is associated to a proper gating strategy to (i) limit the
530 interference of un-target cells in the endpoint analysis, (ii) acquire complementary information (e.g. the mortality
531 induced by phagocytosis activity), and (iii) refine the endpoint measurements (e.g. excluding dead cells for
532 phagocytosis analysis).

533 All these modifications resulted in an operational and rapid protocol to analyze hemocyte mortality and
534 phagocytosis activity in *D. polymorpha* hemocytes. This procedure enhanced the analysis quality as well as the
535 accuracy of the analyzed endpoints. The proposed methodology is particularly adapted to *ex vivo* exposures such
536 as chemical or environmental sample toxicity assessment, but it can also be applied to *in vivo* experiments such
537 as biomonitoring surveys following minor adjustments.

538

539 **Table 1.** Details of the protocol developed for hemocyte ex vivo or in vivo exposure followed by flow cytometry
 540 analysis

# Step	Step details
#1	Hemolymph sampling. Withdrawn hemolymph from mussel muscle with insulin syringe previously rinsed and filled with 50 μL of L15-15% \oplus . Store samples in sterile microtubes in a rack previously placed on ice.
#2	Cell deposit. Determine cell concentration using KOVA [®] slide (or equivalent method). Depose 75×10^3 cell.well ⁻¹ in a 96-well microplate.
#3	Sedimentation. For ex vivo exposure: Keep sample for 20 min at 16 °C for sedimentation. Remove supernatant and add 190 μL L15-15% \oplus . For in vivo exposure: Complete volume in each well to 190 μL with L15-15% \oplus .
#4	Cell contamination and exposure. Add 10 μL of contamination solution or L15-15% \oplus medium (negative controls), and fluorescent beads to reach a 1:50 hemocytes-beads ratio. After homogenization, incubate at 16 °C for 4 h.
#5	Cell detachment. 15 min before the end of the exposure period, transfer each sample supernatant in a new microplate. Add 100 μL of Trypsin-EDTA 1 \times solution in each emptied well and incubate for 10 min at room temperature. Flush and transfer the detached cell suspension to the corresponding sample in the new microplate (i.e. 300 μL total for each sample)
#6	Probe addition. Add 5 μM (final concentration) of Hoechst [®] 33342, homogenize and incubate for 10 min at room temperature. Add 10 $\mu\text{g.mL}^{-1}$ (final concentration) of propidium iodide to each sample and thoroughly homogenize.
#7	Flow cytometric analysis. Samples are analyzed by runs of 4 samples thoroughly mixed by 10-times pipetting just before analysis. Each sample is analyzed for 10,000 events (or Hoechst-positive events when the cellular probe is used) in the hemocyte region (R1) at a flow rate of 66 $\mu\text{L.min}^{-1}$. Hoechst staining is analyzed in FL2 channel (excitation: 375 nm) with a 427/10 nm filter; propidium iodide in FL4 channel (excitation: 375 nm) with a 670 LP filter; YG beads in FL1 channel (excitation: 473 nm) with a 530/30 nm filter attenuated by 90%.

541

542

543 **Acknowledgments**

544 This work was carried out in the framework of the Excellence Project AMISOLVER, supported by the
545 Champagne-Ardenne region (France) and the European Regional Development Fund (ERDF). The authors thank
546 Ph.D. Marc Bonnard from the UMR-I 02 SEBIO in Reims-Champagne-Ardenne University for providing typical
547 cellular profiles of hemolymph individual samples.

548

549 **References**

- 550 Auffret, M., Oubella, R., 1997. Hemocyte aggregation in the oyster *Crassostrea gigas*: In vitro measurement and
551 experimental modulation by xenobiotics. *Comp. Biochem. Physiol. Part A Physiol.* 118, 705–712.
552 doi:10.1016/S0300-9629(97)00017-0
- 553 Binelli, A., Cogni, D., Parolini, M., Riva, C., Provini, A., 2009. In vivo experiments for the evaluation of genotoxic
554 and cytotoxic effects of Triclosan in Zebra mussel hemocytes. *Aquat. Toxicol.* 91, 238–244.
555 doi:10.1016/j.aquatox.2008.11.008
- 556 Binelli, A., Della Torre, C., Magni, S., Parolini, M., 2014. Does zebra mussel (*Dreissena polymorpha*) represent
557 the freshwater counterpart of *Mytilus* in ecotoxicological studies? A critical review. *Environ. Pollut.* 196C,
558 386–403. doi:10.1016/j.envpol.2014.10.023
- 559 Blaise, C., Trottier, S., Gagné, F., Lallement, C., Hansen, P.-D.D., 2002. Immunocompetence of bivalve
560 hemocytes as evaluated by miniaturized phagocytosis assay. *Environ. Toxicol.* 17, 160–169.
561 doi:10.1002/tox.10047
- 562 Brousseau, P., Pellerin, J., Morin, Y., Cyr, D., Blakley, B., Boermans, H., Fournier, M., 1999. Flow cytometry as a
563 tool to monitor the disturbance of phagocytosis in the clam *Mya arenaria* hemocytes following in vitro
564 exposure to heavy metals. *Toxicology* 142, 145–156. doi:10.1016/S0300-483X(99)00165-1
- 565 Chen, J.-H., Bayne, C.J., 1995. Hemocyte adhesion in the California mussel (*Mytilus californianus*): regulation by
566 adenosine. *Biochim. Biophys. Acta - Mol. Cell Res.* 1268, 178–184. doi:10.1016/0167-4889(95)00074-3
- 567 Costa, M.M., Dios, S., Alonso-Gutierrez, J., Romero, A., Novoa, B., Figueras, A., 2009. Evidence of high
568 individual diversity on myticin C in mussel (*Mytilus galloprovincialis*). *Dev. Comp. Immunol.* 33, 162–170.
569 doi:10.1016/j.dci.2008.08.005
- 570 European Commission (EC), 2006. Regulation (EC) No 1907/2006 of the European Parliament and of the Council
571 of 18 December 2006 concerning the Registration, Evaluation, Authorisation and restriction of Chemicals
572 (REACH), establishing a European Chemicals Agency, amending Directive 1999/4. *Off. J. Eur.*
573 *Communities* 1–520. doi:2004R0726 - v.7 of 05.06.2013

574 Evariste, L., Auffret, M., Audonnet, S., Geffard, A., David, E., Brousseau, P., Fournier, M., Betoulle, S., 2016.
575 Functional features of hemocyte subpopulations of the invasive mollusk species *Dreissena polymorpha*.
576 *Fish Shellfish Immunol.* 56, 144–154. doi:10.1016/j.fsi.2016.06.054

577 Evariste, L., David, E., Cloutier, P.-L., Brousseau, P., Auffret, M., Desrosiers, M., Groleau, P.E., Fournier, M.,
578 Betoulle, S., 2018. Field biomonitoring using the zebra mussel *Dreissena polymorpha* and the quagga
579 mussel *Dreissena bugensis* following immunotoxic responses. Is there a need to separate the two species?
580 *Environ. Pollut.* 238, 706–716. doi:10.1016/j.envpol.2018.03.098

581 Evariste, L., Rioult, D., Brousseau, P., Geffard, A., David, E., Auffret, M., Fournier, M., Betoulle, S., 2017.
582 Differential sensitivity to cadmium of immunomarkers measured in hemocyte subpopulations of zebra
583 mussel *Dreissena polymorpha*. *Ecotoxicol. Environ. Saf.* 137, 78–85. doi:10.1016/j.ecoenv.2016.11.027

584 Fournier, M., Cyr, D., Blakley, B., Boermans, H., Brousseau, P., 2000. Phagocytosis as a Biomarker of
585 Immunotoxicity in Wildlife Species Exposed to Environmental Xenobiotics. *Am. Zool.* 40, 412–420.
586 doi:10.1093/icb/40.3.412

587 Goedken, M., De Guise, S., 2004. Flow cytometry as a tool to quantify oyster defence mechanisms. *Fish Shellfish*
588 *Immunol.* 16, 539–552. doi:10.1016/j.fsi.2003.09.009

589 Grandiosa, R., Bouwman, M.-L., Young, T., Mérien, F., Alfaro, A.C., 2018. Effect of antiaggregants on the in vitro
590 viability, cell count and stability of abalone (*Haliotis iris*) haemocytes. *Fish Shellfish Immunol.* 78, 131–139.
591 doi:10.1016/j.fsi.2018.04.038

592 Grandiosa, R., Mérien, F., Pillay, K., Alfaro, A., 2016. Innovative application of classic and newer techniques for
593 the characterization of haemocytes in the New Zealand black-footed abalone (*Haliotis iris*). *Fish Shellfish*
594 *Immunol.* 48, 175–184. doi:10.1016/j.fsi.2015.11.039

595 Hégaret, H., Wikfors, G.H., Soudant, P., 2003. Flow cytometric analysis of haemocytes from eastern oysters,
596 *Crassostrea virginica*, subjected to a sudden temperature elevation. *J. Exp. Mar. Bio. Ecol.* 293, 249–265.
597 doi:10.1016/S0022-0981(03)00235-1

598 Hinzmann, M.F., Lopes-Lima, M., Gonçalves, J., Machado, J., 2013. Antiaggregant and toxic properties of
599 different solutions on hemocytes of three freshwater bivalves. *Toxicol. Environ. Chem.* 95, 790–805.
600 doi:10.1080/02772248.2013.818149

601 Huang, J., Li, S., Liu, Y., Liu, C., Xie, L., Zhang, R., 2018. Hemocytes in the extrapallial space of *Pinctada fucata*
602 are involved in immunity and biomineralization. *Sci. Rep.* 8, 4657. doi:10.1038/s41598-018-22961-y

603 Jones, H.D., 1983. The Circulatory Systems of Gastropods and Bivalves, in: Saleuddin, A.S.M., Wilbur, K.M.
604 (Eds.), *The Mollusca*, Vol. 5. Academic Press, pp. 189–238. doi:10.1016/B978-0-12-751405-5.50012-9

605 Labreuche, Y., Lambert, C., Soudant, P., Boulo, V., Huvet, A., Nicolas, J.L., 2006. Cellular and molecular

606 hemocyte responses of the Pacific oyster, *Crassostrea gigas*, following bacterial infection with *Vibrio*
607 *aestuarianus* strain 01/32. *Microbes Infect.* 8, 2715–2724. doi:10.1016/j.micinf.2006.07.020

608 Ladeiro, M.P., Barjhoux, I., Bigot-Clivot, A., Bonnard, M., David, E., Dedourge-Geffard, O., Geba, E., Lance, E.,
609 Lepretre, M., Magniez, G., Rioult, D., Aubert, D., Villena, I., Daniele, G., Salvador, A., Vulliet, E.,
610 Armengaud, J., Geffard, A., Palos Ladeiro, M., Barjhoux, I., Bigot-Clivot, A., Bonnard, M., David, E.,
611 Dedourge-Geffard, O., Geba, E., Lance, E., Lepretre, M., Magniez, G., Rioult, D., Aubert, D., Villena, I.,
612 Daniele, G., Salvador, A., Vulliet, E., Armengaud, J., Geffard, A., Ladeiro, M.P., Barjhoux, I., Bigot-Clivot,
613 A., Bonnard, M., David, E., Dedourge-Geffard, O., Geba, E., Lance, E., Lepretre, M., Magniez, G., Rioult,
614 D., Aubert, D., Villena, I., Daniele, G., Salvador, A., Vulliet, E., Armengaud, J., Geffard, A., 2017. Mussel as
615 a Tool to Define Continental Watershed Quality, in: Ray, S.B.T.-O. and M.M. (Ed.), *Organismal and*
616 *Molecular Malacology*. InTech, Rijeka, p. Ch. 03. doi:10.5772/67995

617 Le Foll, F., Rioult, D., Boussa, S., Pasquier, J., Dagher, Z., Leboulenger, F., 2010. Characterisation of *Mytilus*
618 *edulis* hemocyte subpopulations by single cell time-lapse motility imaging. *Fish Shellfish Immunol.* 28, 372–
619 386. doi:10.1016/j.fsi.2009.11.011

620 Le Guernic, A., Felix, C., Bigot, A., David, E., Dedourge-Geffard, O., Geffard, A., Betoulle, S., 2015. Food
621 Deprivation and Modulation of Hemocyte Activity in the Zebra Mussel (*Dreissena polymorpha*). *J. Shellfish*
622 *Res.* 34, 423–431. doi:10.2983/035.034.0226

623 Le Guernic, A., Geffard, A., Le Foll, F., Palos Ladeiro, M., 2019. Comparison of viability and phagocytic
624 responses of hemocytes withdrawn from the bivalves *Mytilus edulis* and *Dreissena polymorpha*, and
625 exposed to human parasitic protozoa. *Int. J. Parasitol.*

626 Leprêtre, M., Almunia, C., Armengaud, J., Salvador, A., Geffard, A., Palos-Ladeiro, M., 2019. The immune
627 system of the freshwater zebra mussel, *Dreissena polymorpha*, decrypted by proteogenomics of hemocytes
628 and plasma compartments. *J. Proteomics* 202, 103366. doi:10.1016/j.jprot.2019.04.016

629 Li, X., Cowles, E.A., Cowles, R.S., Gaugler, R., Cox-Foster, D.L., 2009. Characterization of immunosuppressive
630 surface coat proteins from *Steinernema glaseri* that selectively kill blood cells in susceptible hosts. *Mol.*
631 *Biochem. Parasitol.* 165, 162–169. doi:10.1016/j.molbiopara.2009.02.001

632 Luengen, A.C., Friedman, C.S., Raimondi, P.T., Flegal, A.R.R., 2004. Evaluation of mussel immune responses as
633 indicators of contamination in San Francisco Bay. *Mar. Environ. Res.* 57, 197–212. doi:10.1016/S0141-
634 1136(03)00070-9

635 Mersch, J., Beauvais, M.-N., Nagel, P., 1996. Induction of micronuclei in haemocytes and gill cells of zebra
636 mussels, *Dreissena polymorpha*, exposed to clastogens. *Mutat. Res. Toxicol.* 371, 47–55.
637 doi:10.1016/S0165-1218(96)90093-2

638 Okazaki, T., Okudaira, N., Iwabuchi, K., Fugo, H., Nagai, T., 2006. Apoptosis and Adhesion of Hemocytes During

639 Molting Stage of Silkworm, *Bombyx mori*. Zool. Soc. Japan Zool. Sci. 23, 299–304. doi:10.2108/zsj.23.299

640 Quinn, B., Costello, M.J., Dorange, G., Wilson, J.G., Mothersill, C., 2009. Development of an in vitro culture
641 method for cells and tissues from the zebra mussel (*Dreissena polymorpha*). Cytotechnology 59, 121–34.
642 doi:10.1007/s10616-009-9202-3

643 Rebelo, M. de F., Figueiredo, E. de S., Mariante, R.M., Nóbrega, A., de Barros, C.M., Allodi, S., 2013. New
644 Insights from the Oyster *Crassostrea rhizophorae* on Bivalve Circulating Hemocytes. PLoS One 8, e57384.
645 doi:10.1371/journal.pone.0057384

646 Rioult, D., Lebel, J.-M., Le Foll, F., 2013. Cell tracking and velocimetric parameters analysis as an approach to
647 assess activity of mussel (*Mytilus edulis*) hemocytes in vitro. Cytotechnology 65, 749–758.
648 doi:10.1007/s10616-013-9558-2

649 Rioult, D., Pasquier, J., Boulangé-Lecomte, C., Poret, A., Abbas, I., Marin, M., Minier, C., Le Foll, F., 2014. The
650 multi-xenobiotic resistance (MXR) efflux activity in hemocytes of *Mytilus edulis* is mediated by an ATP
651 binding cassette transporter of class C (ABCC) principally inducible in eosinophilic granulocytes. Aquat.
652 Toxicol. 153, 98–109. doi:10.1016/j.aquatox.2013.11.012

653 Sauv , S., Brousseau, P., Pellerin, J., Morin, Y., Sen cal, L., Goudreau, P., Fournier, M., 2002. Phagocytic
654 activity of marine and freshwater bivalves: in vitro exposure of hemocytes to metals (Ag, Cd, Hg and Zn).
655 Aquat. Toxicol. 58, 189–200. doi:10.1016/S0166-445X(01)00232-6

656 Sawai, H., Domae, N., 2011. Discrimination between primary necrosis and apoptosis by necrostatin-1 in Annexin
657 V-positive/propidium iodide-negative cells. Biochem. Biophys. Res. Commun. 411, 569–573.
658 doi:10.1016/j.bbrc.2011.06.186

659 Tanguy, M., McKenna, P., Gauthier-Clerc, S., Pellerin, J., Danger, J.-M., Siah, A., 2013. Functional and molecular
660 responses in *Mytilus edulis* hemocytes exposed to bacteria, *Vibrio splendidus*. Dev. Comp. Immunol. 39,
661 419–429. doi:10.1016/j.dci.2012.10.015

662 Tryphonas, H., Fournier, M., Blakley, B.R., Smits, J.E.G., Brousseau, P. (Eds.), 2005. Investigative
663 immunotoxicology. Taylor & Francis.

664 US EPA, 2007. Pesticides; Data Requirements for Conventional Chemicals, Technical Amendments, and Data
665 Requirements for Biochemical and Microbial Pesticides; Final Rules.

666 Villela, I.V., de Oliveira, I.M., da Silva, J., Henriques, J.A.P., 2006. DNA damage and repair in haemolymph cells
667 of golden mussel (*Limnoperna fortunei*) exposed to environmental contaminants. Mutat. Res. - Genet.
668 Toxicol. Environ. Mutagen. 605, 78–86. doi:10.1016/j.mrgentox.2006.02.006

669 Wallberg, F., Tenev, T., Meier, P., 2016. Time-Lapse Imaging of Cell Death. Cold Spring Harb. Protoc. 2016,
670 pdb.prot087395. doi:10.1101/pdb.prot087395

671 Zuykov, M., Pelletier, E., Harper, D.A.T., 2013. Bivalve mollusks in metal pollution studies: From bioaccumulation
672 to biomonitoring. *Chemosphere* 93, 201–208. doi:10.1016/j.chemosphere.2013.05.001

673

674

675 **A new protocol for the simultaneous flow cytometric analysis of**
676 **cytotoxicity and immunotoxicity on zebra mussel (*Dreissena***
677 ***polymorpha*) hemocytes**

678 Iris Barjhoux^{a,✉}, Damien Rioult^b, Alain Geffard^a, Melissa Palos-Ladeiro^a

679

680 ^a *Université de Reims Champagne-Ardenne, UMR-I-02 Stress Environnementaux et Biosurveillance des milieux*
681 *aquatiques (SEBIO), Reims, France*

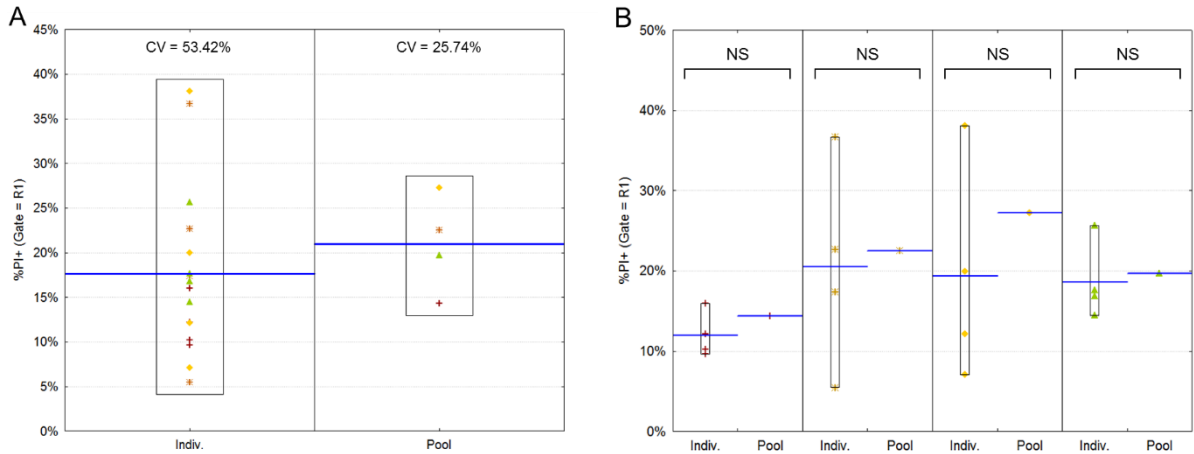
682 ^b *Université de Reims Champagne-Ardenne/Institut national de l'environnement industriel et des risques (Ineris),*
683 *Plateau technique de cytométrie environnementale MOBICYTE*

684

685

Supplementary material

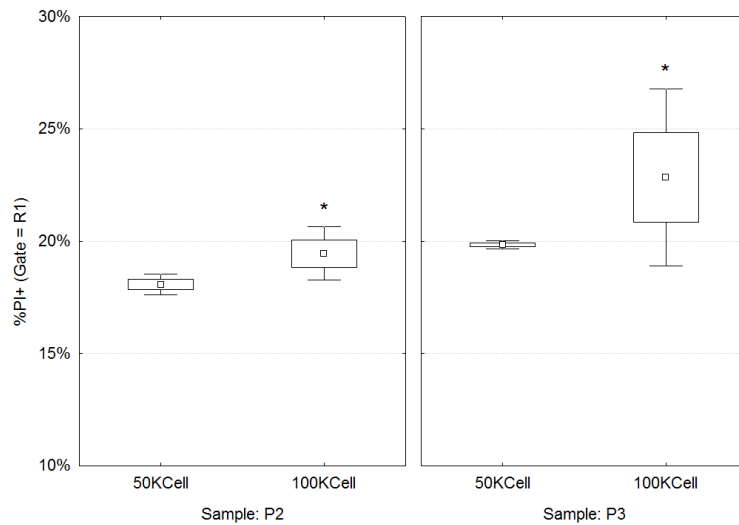
686



687

688 **Figure S1.** Percentage of PI-positive events (%PI+) recorded in hemocyte region (R1) in fresh individual (left) and
 689 pooled (right) samples. (A) Global overview of value distribution for the individual and pooled samples. (B)
 690 Exploded view of the values observed for each pool and the corresponding individual samples. Individual
 691 samples used to make a pooled sample (N = 4) shared the same marker. Horizontal blue lines indicate the mean
 692 value for individual and pooled samples. No significant difference (NS) was observed between individual and pool
 693 values for each set of samples according to the Wilcoxon signed ranks test ($p > 0.05$).

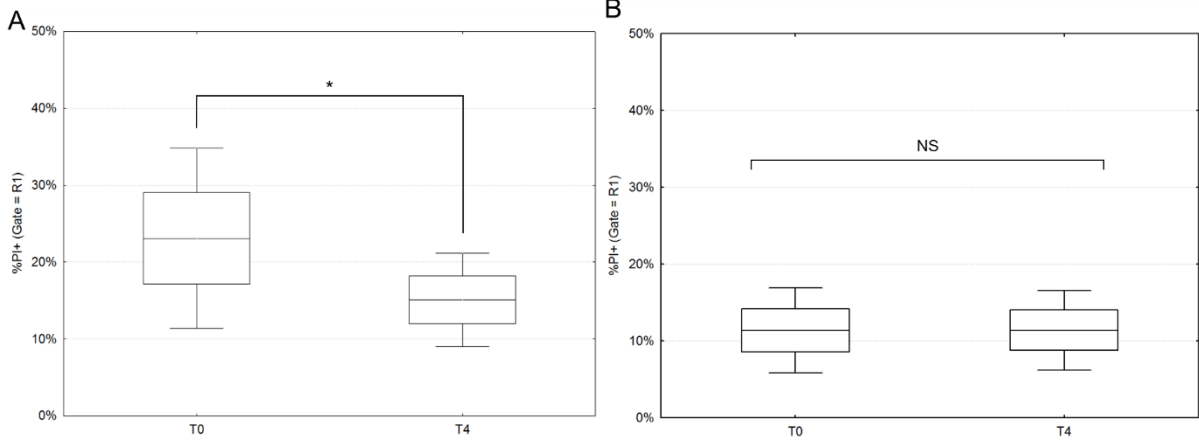
694



695

696 **Figure S2.** Illustration of the effect of the number of cells deposited in microplate on the mortality rate (%PI+)
 697 analyzed by flow cytometry. For each pooled sample (P2 and P3), 50,000 and 100,000 cells were deposited four
 698 times and immediately analyzed for mortality (PI+ events) in hemocyte region (R1) by flow cytometry. Data are
 699 presented as mean value (empty square) \pm standard deviation (box). The whiskers represent the mean value \pm
 700 $1.96 \times$ standard deviation. Asterisks mark significant differences ($p < 0.05$) between %PI+ values observed for
 701 50 KCell and 100 KCell for each sample, according to the non-parametric Mann-Whitney U test.

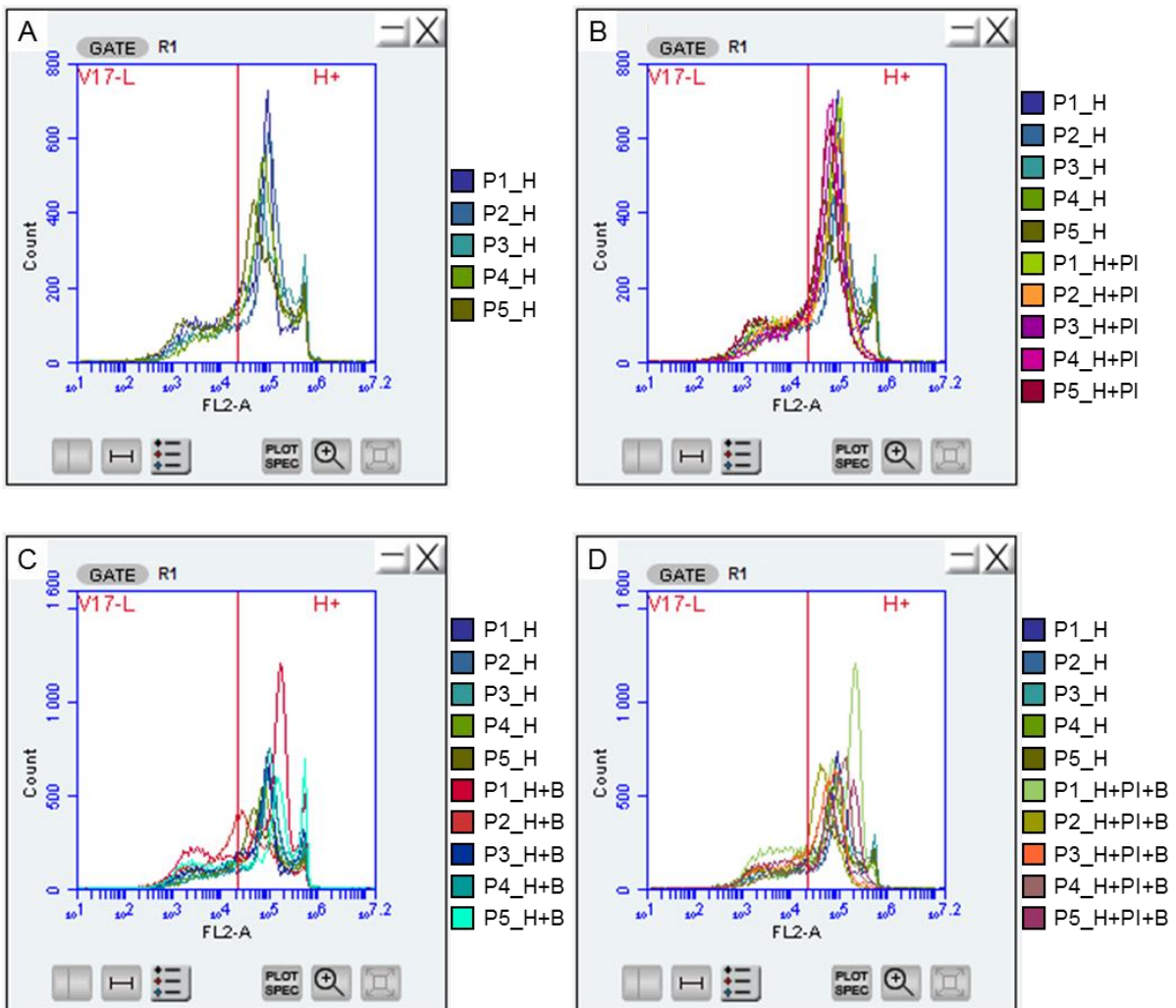
702



703

704 **Figure S3.** Percentage of PI-positive events (%PI+) recorded in hemocyte region (R1) at T0 (fresh) and after 4h-
 705 incubation at 16 °C without (A) or with (B) a sedimentation step before incubation (See part 2.3.1 and Table 1 for
 706 details). Data are presented as mean value (horizontal line) ± SD (box). The whiskers represent the mean value
 707 ± 1.96*SD (N = 10 pools). Asterisks mark significant differences ($p < 0.05$) between T0- and T4-data, according
 708 to the t-test for dependent samples. NS, not significant.

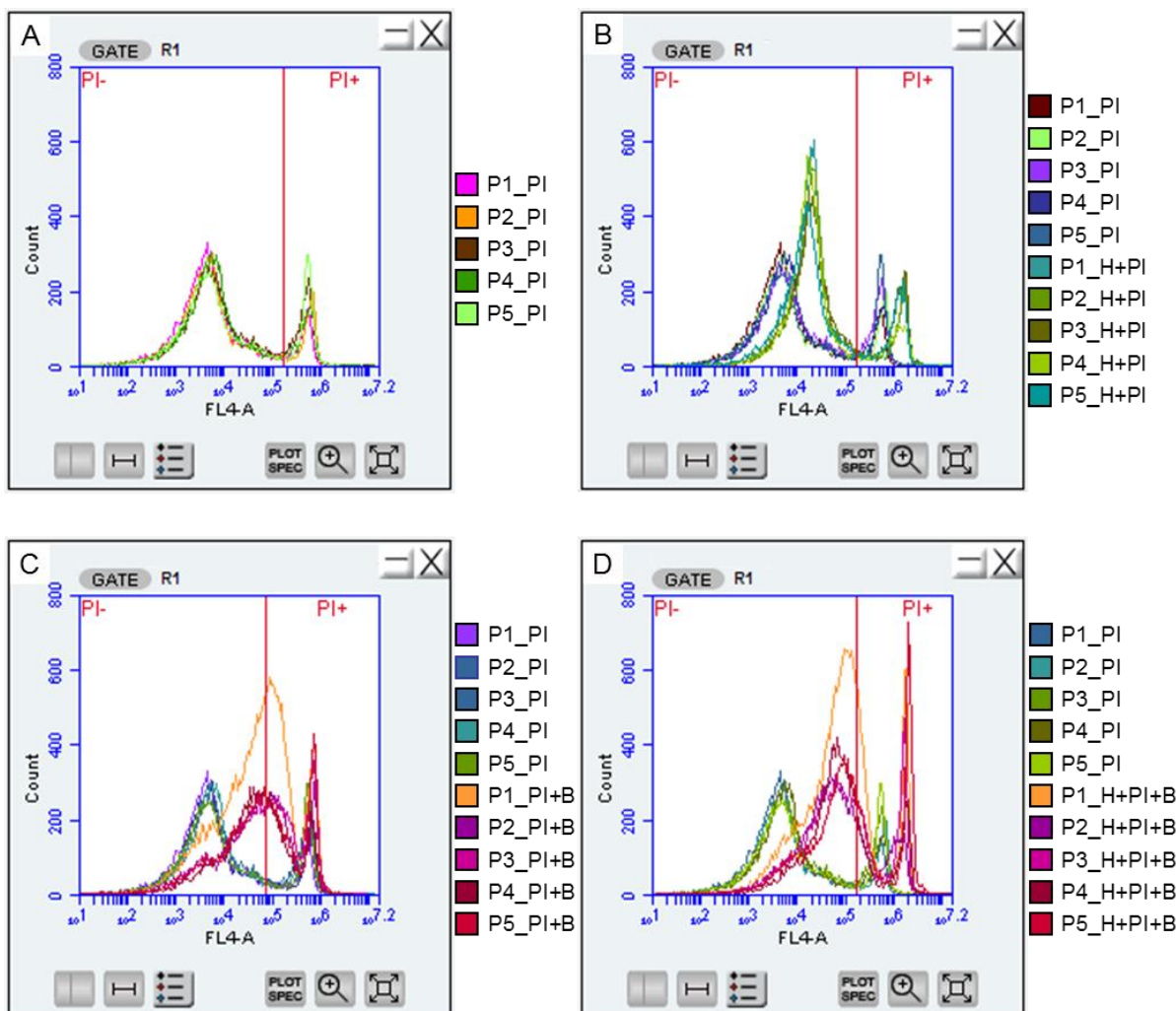
709



710

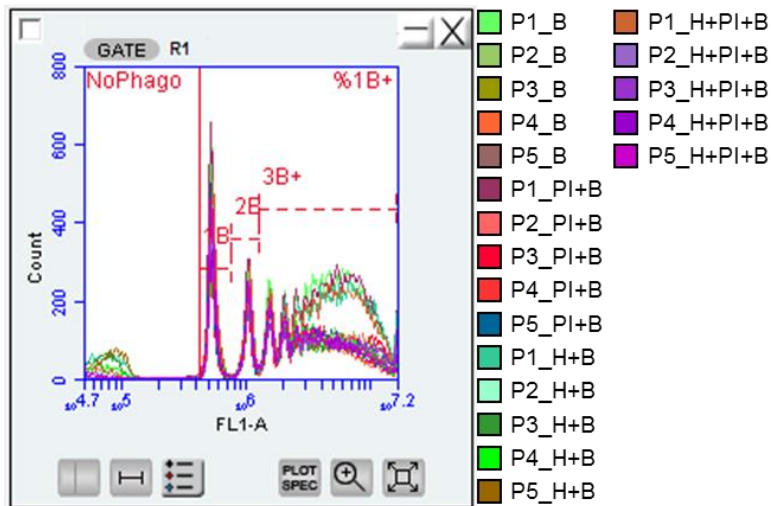
711 **Figure S4.** Fluorescence profiles of Hoechst® 33342 (H) observed in the hemocyte region (R1) after 4h-
 712 incubation at 16 °C for five pooled samples of hemolymph (P1 to P5). To see the effects of multi-labeling
 713 procedure on Hoechst fluorescence profile, the profiles of the samples were superimposed for each probe
 714 combination i.e. Hoechst alone (H, **A to D**), Hoechst and PI (**B**), Hoechst and beads (**H+B, C**) and Hoechst,
 715 PI and beads (**H+PI+B, D**).

716



717

718 **Figure S5.** Fluorescence profiles of propidium iodide (PI) observed in the hemocyte region (R1) after 4h-
 719 incubation at 16 °C for five pooled samples of hemolymph (P1 to P5). To see the effects of multi-labeling
 720 procedure on PI fluorescence profile, the profiles of the samples were superimposed for each probe
 721 combination i.e. PI alone (**A to D**), Hoechst and PI (**H+PI, B**), PI and beads (**PI+B, C**) and Hoechst, PI and beads (**H+PI+B, D**).



722

723 **Figure S6.** Fluorescence profiles of YG beads (B) observed in the hemocyte region (R1) after 4h-incubation at
 724 16 °C for five pooled samples of hemolymph (P1 to P5). To see the effects of multi-labeling procedure on beads
 725 fluorescence profile, the profiles of the samples were superimposed for each probe combination i.e. beads alone
 726 (B), beads and PI (PI+B), Hoechst and beads (H+B) and Hoechst, PI and beads (H+PI+B).

727

728

729